Submitted to ADVANCED ENERGY MATERIALS

DOI: 10.1002/((please add manuscript number))
Article type: Communication

Solid Electrolyte: the Key for High-Voltage Lithium Batteries

*Juchuan Li *, Cheng Ma, Miaofang Chi, Chengdu Liang, and Nancy J. Dudney **

Dr. Juchuan Li, Dr. Nancy J. Dudney
Materials Science & Technology Division, Oak Ridge National Laboratory
Oak Ridge, TN, 37831, USA
Email: lij2@ornl.gov; dudneynj@ornl.gov

Dr. Cheng Ma, Dr. Miaofang Chi, Dr. Chengdu Liang
Center for Nanophase Materials Sciences, Oak Ridge National Laboratory
Oak Ridge, TN, 37831, USA

Keywords: high-voltage cathode, $LiNi_{0.5}Mn_{1.5}O_4$ spinel, solid electrolyte (Lipon), lithium-ion battery, solid-state battery

Lithium batteries with increased energy density are required for the fast growing markets of mobile electronic devices, electric vehicles, and smart grids. Lithium batteries with high energy density can be realized by utilizing cathodes with either high capacity or high voltage. While inventing high-capacity cathodes usually requires exploring new compound and phases, high-voltage cathodes can be designed relatively easily by cation substitution in existing compounds, without altering much the crystal structures or the intercalation chemistry. [1, 2] For example, by partial substituting the Mn cations in $LiMn_2O_4$ with other transition metals, the operating potential of the spinel-type cathodes can be increased from 4.0 V for the $Mn^{3+/4+}$ couple to 4.7 V, 4.8 V, and 5.1 V for the $Ni^{2+/4+}$, $Cr^{3+/4+}$, and $Fe^{3+/4+}$ couples, respectively. [3]

Although these high-voltage cathodes could potentially increase the energy density of Lithium batteries by 20~50%, the practical use of high-voltage Lithium batteries is hampered by the intrinsic problems of the conventional batteries: narrow electrochemical window of the liquid electrolyte, dissolution of transition metals from the cathode, and poor safety of the liquid electrolyte and Li anode. The high operating voltages of the aforementioned cathode compounds are beyond the voltage window of the carbonate-based electrolyte, ~4.5 V; thus, the electrolyte undergoes apparently continuous oxidative decomposition during cycling and forms non-passivating solid electrolyte interphases (SEI) films on cathodes. As a result, low coulombic efficiency is usually observed for high-voltage cathode based half cells (where Li supply is abundant), [4-6, 7] and the cycle life of high-voltage full cells (where the amount of Li ions is limited) is dramatically limited. [4, 8, 9] Also, the non-passivating athode SEI films result in chemical etching of the cathodes by electrolytes and dissolution of transition metal ions. [9, 10] These dissolved transition metals decrease the available capacity in cathodes and increase the thickness of anode SEI films. [9] Furthermore, safety is a great concern for high-voltage LIBs, where the electrolytes, containing flammable esters and ethers, are operated beyond their stable voltage limits. Lastly, lithium batteries with Li metal anodes are abandoned because of the notorious problem of Li dendrite growth [11] and lithium-ion batteries with graphitic anodes are commercially used at the cost of much lowered capacity and operating voltage. Although tremendous research efforts have been devoted to developing new electrolytes with expanded safety window [5, 12] as well as modifying the surface of anodes [13] and cathodes [7, 10, 14] for improved stability, it is not easy to address the above four problems simultaneously. High-voltage lithium batteries can be successfully utilized only if all these problems associated with the cathode, the electrolyte, and the anode are solved fully.

It is well known that many solid electrolytes have a voltage window beyond 5 V and thus do not decompose under cathodic current, such as $Li_{10}GeP_2S_{12}$, [15] Li_3PS_4, [16] Li_4SnS_4, [17]

$Li_7La_3Zr_2O_{12}$, [18] and lithium phosphorus oxynitride (Lipon). [19] Furthermore, with a solid electrolyte, the concern of transition metal dissolution into the electrolyte is minimal. Compared with carbonate electrolytes, most ceramic solid electrolytes are intrinsically non-flammable. Lastly, lithium metal is compatible with many solid electrolytes and is less likely to form dendrites during cycling because of the mechanical robustness of the solid electrolyte. [20] The prominent problem of solid-state batteries is their low power densities compared with liquid-electrolyte lithium batteries, resulting from the low ionic conductivity of the solid electrolyte, the electrode/electrolyte interfacial compatibility, and limited kinetics of the electrodes. [21, 22] The recently discovered solid electrolytes with high ionic conductivity enable the possibility of fabricating solid-state lithium batteries with a power performance comparable to that of liquid-electrolyte batteries. [15, 23] On the other hand, interfacial instability between the electrode and electrolyte is a great challenge for solid-state batteries. [15, 17, 24, 25] Proper engineering at the interfaces of electrode/electrolyte is required for good cycling performance of most solid-state lithium batteries. [15, 24, 26, 27] Can solid-state batteries fundamentally tackle all the problems in high-voltage lithium batteries, the unstable cathodes, electrolytes, and anodes?

In this work, we demonstrate the possibility to realize high-voltage cycling in solid-state systems using an example of $LiNi_{0.5}Mn_{1.5}O_4$ cathode, Lipon solid electrolyte, and Li metal anode. Disordered spinel phase $LiNi_{0.5}Mn_{1.5}O_4$ (theoretical capacity 147 mAh g^{-1}) is one of the most attractive high-voltage cathodes because of its high operating voltage of ~4.7 V, stable structure, and superior kinetics over ordered $LiNi_{0.5}Mn_{1.5}O_4$. [2, 28] Lipon is used as the model solid electrolyte mainly because of its wide voltage window (0~5.5 V) [19] and excellent interfacial compatibility with both cathodes and anodes. [19, 29] Fabrication of thin-film battery with $LiNi_{0.5}Mn_{1.5}O_4$ cathode has been challenging, [30] and this work demonstrate the first successful application of $LiNi_{0.5}Mn_{1.5}O_4$ cathode in solid-state battery. Our results

show that the solid-state high-voltage lithium battery delivers an outstanding cycling performance with 90% capacity retention after 10,000 cycles while the amount of electrolyte is thousands of times less than that in liquid-electrolyte batteries. Compared with liquid-electrolyte batteries, the electrolyte decomposition in solid-state lithium battery is minimum, resulting in high coulombic efficiency of 99.98% and a fraction of 1/125 cumulative charge loss.

A solid electrolyte with a sufficiently wide electrochemical window does not decompose when cycled to high voltage. **Figure 1a** shows the capacity retention of $LiNi_{0.5}Mn_{1.5}O_4$ cathode in a solid-state battery with Lipon electrolyte and Li metal anode cycled between 5.1 V and 3.5 V at 5C. The high coulombic efficiency of the solid-state battery exceeds 99.98%, as shown in Figure 1b, indicating that the decomposition of solid electrolyte is minimum. In sharp contrast, the coulombic efficiency of a lithium battery with identical cathode and a common liquid electrolyte (1.2 M $LiPF_6$ in EC/DMC, 1:2 by vol.), also cycled at 5C, is below 99.5% (Figure 1b), resulting from the fact that more than 0.5% of the charge is consumed by electrochemical decomposition of the electrolyte in each cycle. The impact of the different electrolyte decomposition is more obvious when we consider the cumulative irreversible charge loss (Figure 1c): the charge loss accumulated for 1,000 cycles for the solid-state battery is 7.9 mAh g^{-1} (per gram of $LiNi_{0.5}Mn_{1.5}O_4$), 125 times smaller than that in the liquid-electrolyte battery (985 mAh g^{-1}). The actual time used for cycling of the solid-state lithium batteries is about 70% of the times for cycling liquid-electrolyte batteries. Charge loss should obviously be minimized for batteries; the huge irreversible charge loss in liquid-electrolyte batteries consumes the solvent and/or lithium salt in the electrolyte, and is particularly detrimental to the life of full cells with limited amount of lithium ions. Furthermore, energy

storage devices with low coulombic efficiency consume extra charge and energy, and are unwanted for long-life applications, such as stationary energy storage.

With a solid electrolyte of wide voltage window, high-voltage lithium batteries can deliver stable capacity for a long life. As shown in Figure 1a, the reversible capacity delivered by the solid-state lithium battery with $LiNi_{0.5}Mn_{1.5}O_4$ cathode is stable for 10,000 cycles, and the capacity retention is 90.6% after 10,000 cycles, corresponding to a decay of less than 0.001% per cycle. Exact cause of this decay is not identified here, but from comparison to 96% retention at lower current (fig.1d) the loss is due to slowly increasing resistance in the cell. The reversible capacity of the solid-state batteries under C/10 is about 120 mAh g^{-1}, corresponding to ~82% of its theoretical capacity. The round trip energy efficiency is greater than 97%. For most applications, such a battery has a cycle life longer than most devices, and can be used for a lifetime without maintenance. The solid electrolyte does not alter the intercalation chemistry of $LiNi_{0.5}Mn_{1.5}O_4$, indicated by the voltage profile in Figure 1d and differential voltage-capacity profiles in Figure S1, similar as that of conventional liquid-electrolyte batteries. The first cycle irreversible capacity is mostly caused by the redox couple Mn^{3+}/Mn^{4+} instead of electrolyte decomposition, evidenced by the fact that the capacity of the 4 V plateau (~40 mAh g^{-1}) equals to the 1st cycle irreversible capacity. The as-deposited cathode material contains excess Li, which is removed during the first charging process and does not intercalate above the cutoff voltage of 3 V. After the first cycle, the voltage-capacity profiles are almost identical for the subsequent cycles through at least 10,000 cycles. On the other hand, decomposition of liquid electrolyte is the limit for high-voltage lithium batteries, and the cycle life of a high-voltage liquid-electrolyte battery directly depends on the amount of electrolyte, as shown in Figure 1a. When charged to high voltage, the oxidative decomposition of electrolyte leads to reduced amount of mobile Li ions. Furthermore, EC undergoes polymerization and increases the viscosity of the electrolyte gradually. [31] These

two facts lead to gradual decrease in the conductivity of the electrolyte, and eventually the death of a battery. Note that the cycling performance of liquid-electrolyte batteries in Figure 1a are obtained using half cells; full cells (lithium-ion batteries) with $LiNi_{0.5}Mn_{1.5}O_4$ high-voltage cathode and liquid electrolyte will die even faster due to the limited supply of lithium. Furthermore, as shown in **Table 1**, in the example of Liquid-electrolyte Battery 3, the extended cycle life is achieved at the cost of additional electrolyte, occupying 4,100 times the volume of the cathode. Using large amount of liquid electrolyte could greatly lower the total energy density and is not a solution for high-voltage lithium batteries. In solid-state lithium batteries, the amount solid electrolyte can be greatly reduced while maintaining outstanding cycle life, as shown in Table 1.

The issue of transition metal dissolution is naturally eliminated in solid-state lithium batteries where there is no mobile solvent molecule. The identical voltage capacity profiles in Figure 1d supports our assumption that there is little or no transition metal dissolution from the cathode, as this would likely alter the voltage profile or decrease the reversible capacity. A FIB machined SEM cross section is shown in **Figure 2** for the of the $LiNi_{0.5}Mn_{1.5}O_4$/Lipon/Li solid-state battery after 1,000 cycles. The electrode-Lipon interfaces in the image are clearly smooth and adherant. Although the elemental mapping lacks sufficient resolution for good concentration profiles, it is clear that Mn is confined to the cathode side and the Li anode remains dense and smooth with no roughening of the interface. On the other hand, with liquid electrolytes, Mn dissolution is a well-known problem for $LiNi_{0.5}Mn_{1.5}O_4$ cathode and it has been confirmed experimentally that Mn metal migrates to the surface of anodes and participates in the formation of anode SEI. [5, 9, 32]

Smooth Li/Lipon interface can be seen from SEM morphology in Figure 2. Li metal cannot be used in liquid-electrolyte lithium batteries for extended cycling because of the widely known phenomenon of Li dendrite growth, which could cause short circuit of the cell. [13, 33] In our

solid-state lithium battery, Lipon is mechanically robust, and acts as a rigid barrier against the possible growth of Li dendrite. Furthermore, as the top layer of the battery, Li metal can expand freely during cycling and tolerate the volume expansion which is over 200 nm in thickness. [34] The interface between Lipon and Li anode remain smooth, confirming that Li anode can be safely used in solid-state batteries.

The interfacial compatibility between electrode/electrolyte directly determines the performance of solid-state batteries. For many solid electrolytes such as $Li_{10}GeP_2S_{12}$ and Li_2S-P_2S_5, a highly resistive layer forms at the electrode/electrolyte interfaces as a result of interfacial heterojunctions of two ionic conductors. [24, 35]. An "interfacial buffer layer" is usually needed for good performance of such solid-state batteries. [15, 24, 27] In this work, the electrode/electrolyte interfacial compatibility is quantitatively investigated using electrochemical impedance spectroscopy (EIS) at different cycles, as shown in **Figure 3**. The Nyquist plot mainly consists of a semicircle at high frequency representing the interfacial resistance and capacitance as well as ionic resistance of the Lipon electrolyte, and a ~45° line at medium and low frequency representing diffusion-related behaviors. We use the equivalent circuit in Figure S2 to fit the EIS data, and the area specific impedance (ASI) resulting from the high-frequency semicircle is shown in Figure 2b. The ASI of the solid-state battery is 203 $\Omega \cdot cm^2$ after the first cycle, and increased to 229 $\Omega \cdot cm^2$ after 4000 cycles, corresponds to an average increase of a 0.003% per cycle. Noticing that the ASI here is a combined result of the cathode/electrolyte and anode/electrolyte interfaces as well ionic resistance from Lipon electrolyte, the actual electrode/electrolyte interfacial resistance is estimated to be about half of values reported in Figure 2b. Contradictory to a previous report, [30] our results indicate that both the interfaces are stable and Lipon enables the cycling of both $LiNi_{0.5}Mn_{1.5}O_4$ cathode and Li anode. Furthermore, Lipon can be used to build the "interfacial buffer layer" for other solid-state systems.

The bottleneck of solid-state lithium batteries, compared with liquid-electrolyte batteries, is their low power density, [21, 36] resulting from low ionic conductivity of solid electrolytes, limited diffusion kinetics in the electrodes, as well as high interfacial resistance. The problem of low conductivity for the solid electrolytes can be partially solved by reducing the thickness of electrolyte. In our example, the ionic conductivity of the Lipon solid electrolyte is 2×10^{-6} S cm^{-1}, much lower than that of the carbonate liquid electrolyte. However, the electrolyte ionic resistance is compensated by reducing the thickness of the electrolyte to 1 μm. Beyond the ionic conduction, reducing the electrolyte thickness is also beneficial for the overall energy density of the battery. The discharge capacity of the solid-state lithium battery was tested under different rates, as shown in **Figure 4**. Before each measurement, the cell was charged at a slow rate of C/10. The reversible capacity under C/10 rate is 122 mAh g^{-1}. With increased current density, the utilization of active materials decreases slowly because of polarization. Under a relatively fast rate of 10C (1470 mA g^{-1}), a reversible capacity of 90 mAh g^{-1} can be delivered, 74% capacity with respect to that at C/10 (122 mAh g^{-1}). The good rate performance of the solid-state lithium battery in this work is a result of reduced thickness of the electrolyte, good interfacial compatibility, as well as fast kinetics of the disordered $LiNi_{0.5}Mn_{1.5}O_4$ cathode. Lipon allows the investigation of proof-of-principle for solid-state high-voltage lithium batteries. With the emerging of solid electrolytes with both higher ionic conductivity and higher throughput manufacturing than achievable with Lipon, the high power performance of solid-state lithium batteries will be further improved.

In summary, we propose reexamination of high energy density lithium batteries coupling high-voltage cathode with a metallic Li anode via a solid electrolyte. We demonstrate that solid-state system enables the full utilization of high-voltage lithium batteries by solving all the problems with conventional batteries using liquid electrolyte: unstable electrolyte,

dissolution of transition metals from the cathode, and serious safety issues associated with the flammability of the electrolyte and the roughening of the Li metal anode. In our example, the solid-state high-voltage battery consists of $LiNi_{0.5}Mn_{1.5}O_4$ cathode, Lipon electrolyte, and Li metal anode. This solid-state lithium battery delivers remarkable capacity retention of 90% over 10,000 cycles, a round trip energy efficiency of 97% and a high coulombic efficiency of 99.98%, indicating that such batteries can be used for lifetime of most devices without maintenance. This work infuses a new life into existing chemistry of high-voltage lithium batteries.

Compared with liquid-electrolyte lithium batteries, the bottleneck of solid-state batteries is their poor performance under high power and high current. The solid-state lithium battery in this work delivers a good rate-performance because of reduced thickness of the electrolyte, good interfacial stability, and fast kinetics of the electrodes. However, the active loading of cathode is about 0.5 mg cm^{-2}, about 10 times smaller than that in commercial liquid-electrolyte lithium-ion batteries. Future research should be focused on increasing the loading of active materials, utilizing solid electrolyte with high conductivity, engineering composite electrodes for improved kinetics, and reducing the amount of electrolyte for increased energy density of the whole batteries.

Experimental Section

Materials Fabrication: Pt current collector (100 nm thick) and $LiNi_{0.5}Mn_{1.5}O_4$ thin-film cathodes (1 µm thick) were deposited onto alumina plates by DC and RF-magnetron sputtering, repsctively. The active loading of cathodes is 0.45 mg cm^{-2}. The $LiNi_{0.5}Mn_{1.5}O_4$ films were annealed at 700 ºC in air for 1 hour to form the disordered spinel phase. Lipon electrolyte was deposited by RF-magnetron sputtering of a home-made Li_3PO_4 target in reactive N_2 atmosphere (99.9995%). Pure Li metal of 500 nm was deposited as the anode and current collector by thermal evaporation forming a contact to Cu films of 100 nm which were used as the leads. Note that this thickness of Li provides only ~140% excess capacity compare to that of $LiNi_{0.5}Mn_{1.5}O_4$. Cells were sealed in pure Ar during cycling, with no additional Li protection. For the liquid-electrolyte batteries, $LiNi_{0.5}Mn_{1.5}O_4$ electrodes with the same thickness (1 µm) on Pt coated alumina discs were used as working electrodes and pure Li foils (380 µm) were used as the counter electrodes in CR-2032 coin cells. One piece of a polypropylene separator (Celgard 2325) was used in each cell. The electrolyte was 1.2 M $LiPF_6$ dissolved in a solution of ethylene carbonate/dimethyl carbonate (EC/DMC, 1:2 by vol., Novolyte).

Electrochemical Measurement: Solid-state lithium batteries were cycled under constant current of 5C between 3.5 V and 5.1 V using a Bio-Logic VMP3 potentiostat. The battery was slowly cycled under C/10 at every 1000th cycle. Liquid-electrolyte batteries were cycled between 3.5 V and 5 V under a rate of 5C using a Maccor 4000 Series battery cycler . All measurements were carried out at room temperature (23°C), and the capacity is reported based on the mass of $LiNi_{0.5}Mn_{1.5}O_4$ for both solid and liquid lithium batteries. The cycling rate is calculated based on the mass of cathodes, and 1 C corresponds to a current density of 148 mA g^{-1}. EIS measurement was carried out using a VMP3 potentiostat, and the frequency was ramped from 1 MHz to 0.1 mHz with a voltage amplitude of 10 mV. Impedance was

collected at the discharged state (3.5 V). Cells were discharged slowly under a rate of C/20 and before the EIS measurement.

Materials Characterization: After cycling, the cross section of the solid-state lithium battery was examined using a Hitachi NB-5000 dual (Focused Ion/Electron) beam microscope. The specimen was prepared by a standard focused-ion-beam (FIB) lift-out technique with a final thinning voltage of 5 kV. The scanning electron microscopy (SEM) imaging and the associated energy-dispersive X-ray spectroscopy (EDX) measurement were performed at an acceleration voltage of 20 kV.

Supporting Information

Supporting Information is available from the Wiley Online Library or from the authors.

Acknowledgements

This work was supported by the U.S. Department of Energy, Office of Science, Basic Energy Sciences, Materials Sciences and Engineering Division.

Received: ((will be filled in by the editorial staff))
Revised: ((will be filled in by the editorial staff))
Published online: ((will be filled in by the editorial staff))

References

[1]. A. Kraytsberg, Y. Ein‐Eli, *Advanced Energy Materials* **2012**, 2, 922; C.-X. Zu, H. Li, *Energy & Environmental Science* **2011**, 4, 2614; B. C. Melot, J.-M. Tarascon, *Accounts of chemical research* **2013**, 46, 1226.

[2]. M. Hu, X. Pang, Z. Zhou, *Journal of Power Sources* **2013**, 237, 229.

[3]. D. Liu, W. Zhu, J. Trottier, C. Gagnon, F. Barray, A. Guerfi, A. Mauger, H. Groult, C. Julien, J. Goodenough, *RSC Advances* **2014**, 4, 154; Q. M. Zhong, A. Bonakdarpour, M. J. Zhang, Y. Gao, J. R. Dahn, *Journal of the Electrochemical Society* **1997**, 144, 205; C. Sigala, A. Verbaere, J. L. Mansot, D. Guyomard, Y. Piffard, M. Tournoux, *Journal of Solid State Chemistry* **1997**, 132, 372; H. Shigemura, M. Tabuchi, H. Kobayashi, H. Sakaebe, A. Hirano, H. Kageyama, *Journal of Materials Chemistry* **2002**, 12, 1882.

[4]. R. Verrelli, J. Hassoun, A. Farkas, T. Jacob, B. Scrosati, *Journal of Materials Chemistry A* **2013**, 1, 15329.

[5]. N. P. Pieczonka, L. Yang, M. P. Balogh, B. R. Powell, K. Chemelewski, A. Manthiram, S. A. Krachkovskiy, G. R. Goward, M. Liu, J.-H. Kim, *the Journal of Physical Chemistry C* **2013**, 117, 22603.

[6]. S. Li, C. Chen, J. Camardese, J. Dahn, *Journal of the Electrochemical Society* **2013**, 160, A1517; X. Wu, S. Wang, X. Lin, G. Zhong, Z. Gong, Y. Yang, *Journal of Materials Chemistry A* **2014**, 2, 1006.

[7]. S. Brutti, G. Greco, P. Reale, S. Panero, *Electrochimica Acta* **2013**, 106, 483.

[8]. J. Arrebola, A. Caballero, J. Gómez-Cámer, L. Hernán, J. Morales, L. Sánchez, *Electrochemistry Communications* **2009**, 11, 1061; H. Xiang, X. Zhang, Q. Jin, C. Zhang, C. Chen, X. Ge, *Journal of Power Sources* **2008**, 183, 355; B. Guo, X. Yu, X.-G. Sun, M. Chi, Z.-A. Qiao, J. Liu, Y.-S. Hu, X.-Q. Yang, J. B. Goodenough, S. Dai, *Energy & Environmental Science* **2014**,

[9]. N. P. Pieczonka, Z. Liu, P. Lu, K. L. Olson, J. Moote, B. R. Powell, J.-H. Kim, *the Journal of Physical Chemistry C* **2013**, 117, 15947.

[10]. Y. K. Sun, Y. S. Lee, M. Yoshio, K. Amine, *Electrochemical and Solid State Letters* **2002**, 5, A99.

[11]. M. Armand, J. M. Tarascon, *Nature* **2008**, 451, 652.

[12]. L. Hu, Z. Zhang, K. Amine, *Electrochemistry Communications* **2013**, 35, 76; Z. Zhang, L. Hu, H. Wu, W. Weng, M. Koh, P. C. Redfern, L. A. Curtiss, K. Amine, *Energy & Environmental Science* **2013**, 6, 1806.

[13]. F. Ding, W. Xu, G. L. Graff, J. Zhang, M. L. Sushko, X. Chen, Y. Shao, M. H. Engelhard, Z. Nie, J. Xiao, *Journal of the American Chemical Society* **2013**, 135, 4450.

[14]. J. Liu, A. Manthiram, *Chemistry of Materials* **2009**, 21, 1695; D. Liu, J. Trottier, P. Charest, J. Fréchette, A. Guerfi, A. Mauger, C. Julien, K. Zaghib, *Journal of Power Sources* **2012**, 204, 127; J. Li, L. Baggetto, S. K. Martha, G. M. Veith, J. Nanda, C. Liang, N. J. Dudney, *Advanced Energy Materials* **2013**, 3, 1275; S.-X. Zhao, X.-F. Fan, Y.-F. Deng, C.-W. Nan, *Electrochimica Acta* **2012**, 65, 7; K. Yang, L. Z. Fan, J. Guo, X. H. Qu, *Electrochimica Acta* **2012**, 63, 363.

[15]. N. Kamaya, K. Homma, Y. Yamakawa, M. Hirayama, R. Kanno, M. Yonemura, T. Kamiyama, Y. Kato, S. Hama, K. Kawamoto, *Nat. Mater.* **2011**, 10, 682.

[16]. Z. Liu, W. Fu, E. A. Payzant, X. Yu, Z. Wu, N. J. Dudney, J. Kiggans, K. Hong, A. J. Rondinone, C. Liang, *Journal of the American Chemical Society* **2013**, 135, 975.

[17]. G. Sahu, Z. Lin, J. Li, Z. Liu, N. Dudney, C. Liang, *Energy & Environmental Science* **2014**, 7, 1053.

[18]. E. Rangasamy, G. Sahu, J. Keum, A. Rondinone, N. Dudney, C. Liang, *Journal of Materials Chemistry A* **2014**, 2, 4111.
[19]. N. J. Dudney, *Materials Science and Engineering: B* **2005**, 116, 245.
[20]. X. Yu, J. Bates, G. Jellison, F. Hart, *Journal of the Electrochemical Society* **1997**, 144, 524; E. Herbert, W. E. Tenhaeff, N. J. Dudney, G. Pharr, *Thin Solid Films* **2011**, 520, 413; J. J. Xu, D. Xu, Z. L. Wang, H. G. Wang, L. L. Zhang, X. B. Zhang, *Angewandte Chemie International Edition* **2013**, 52, 3887.
[21]. K. Takada, *Acta Materialia* **2013**, 61, 759.
[22]. A. Patil, V. Patil, D. Wook Shin, J.-W. Choi, D.-S. Paik, S.-J. Yoon, *Materials Research Bulletin* **2008**, 43, 1913.
[23]. T. Uemura, K. Goto, M. Ogawa, K. Harada, *Journal of Power Sources* **2013**, 240, 510.
[24]. K. Takada, N. Ohta, L. Zhang, K. Fukuda, I. Sakaguchi, R. Ma, M. Osada, T. Sasaki, *Solid State Ionics* **2008**, 179, 1333.
[25]. A. Brazier, L. Dupont, L. Dantras-Laffont, N. Kuwata, J. Kawamura, J.-M. Tarascon, *Chemistry of Materials* **2008**, 20, 2352.
[26]. K. Takahashi, K. Hattori, T. Yamazaki, K. Takada, M. Matsuo, S. Orimo, H. Maekawa, H. Takamura, *Journal of Power Sources* **2013**, 226, 61.
[27]. J. H. Woo, J. E. Trevey, A. S. Cavanagh, Y. S. Choi, S. C. Kim, S. M. George, K. H. Oh, S.-H. Lee, *Journal of the Electrochemical Society* **2012**, 159, A1120.
[28]. K. M. Shaju, P. G. Bruce, *Dalton Transactions* **2008**, 5471; S. H. Choi, Y. J. Hong, Y. C. Kang, *Nanoscale* **2013**, 5, 7867; J. Xiao, X. L. Chen, P. V. Sushko, M. L. Sushko, L. Kovarik, J. J. Feng, Z. Q. Deng, J. M. Zheng, G. L. Graff, Z. M. Nie, D. W. Choi, J. Liu, J. G. Zhang, M. S. Whittingham, *Advanced Materials* **2012**, 24, 2109.
[29]. B. Wang, J. Bates, F. Hart, B. Sales, R. Zuhr, J. Robertson, *Journal of the Electrochemical Society* **1996**, 143, 3203; B. Fleutot, B. Pecquenard, H. Martinez, M. Letellier, A. Levasseur, *Solid State Ionics* **2011**, 186, 29; Y. Hamon, A. Douard, F. Sabary, C. Marcel, P. Vinatier, B. Pecquenard, A. Levasseur, *Solid State Ionics* **2006**, 177, 257.
[30]. C. Yada, A. Ohmori, K. Ide, H. Yamasaki, T. Kato, T. Saito, F. Sagane, Y. Iriyama, *Advanced Energy Materials* **2014**, 4, 1301416.
[31]. L. Yang, B. Ravdel, B. L. Lucht, *Electrochemical and Solid-State Letters* **2010**, 13, A95.
[32]. Y. Kim, N. J. Dudney, M. Chi, S. K. Martha, J. Nanda, G. M. Veith, C. Liang, *Journal of Electrochemical Society* **2013**, 160, A3113.
[33]. C. M. Lopez, J. T. Vaughey, D. W. Dees, *Journal of the Electrochemical Society* **2009**, 156, A726.
[34]. B. Neudecker, N. Dudney, J. Bates, *Journal of the Electrochemical Society* **2000**, 147, 517; N. Kuwata, J. Kawamura, K. Toribami, T. Hattori, N. Sata, *Electrochemistry Communications* **2004**, 6, 417.
[35]. N. Sata, K. Eberman, K. Eberl, J. Maier, *Nature* **2000**, 408, 946.
[36]. G. Delaizir, V. Viallet, A. Aboulaich, R. Bouchet, L. Tortet, V. Seznec, M. Morcrette, J. M. Tarascon, P. Rozier, M. Dollé, *Advanced Functional Materials* **2012**, 22, 2140.

Tables and Captions

Table 1. Capacity retention vs. the amount of electrolyte for liquid-electrolyte and solid-state batteries. The volume of electrolyte is mormalized to the volume of $LiNi_{0.5}Mn_{1.5}O_4$ cathode.

Cell Number	Volume of electrolyte	Cycle number for 90% retention	Cycle number for 70% retention
Liquid 1	309	148	234
Liquid 2	1340	673	1,423
Liquid 3	1649	1,030	2,029
Liquid 4	4124	3,044	6,085
Solid-state	**1**	**>10,000**	**>10,000**

Figures and Captions

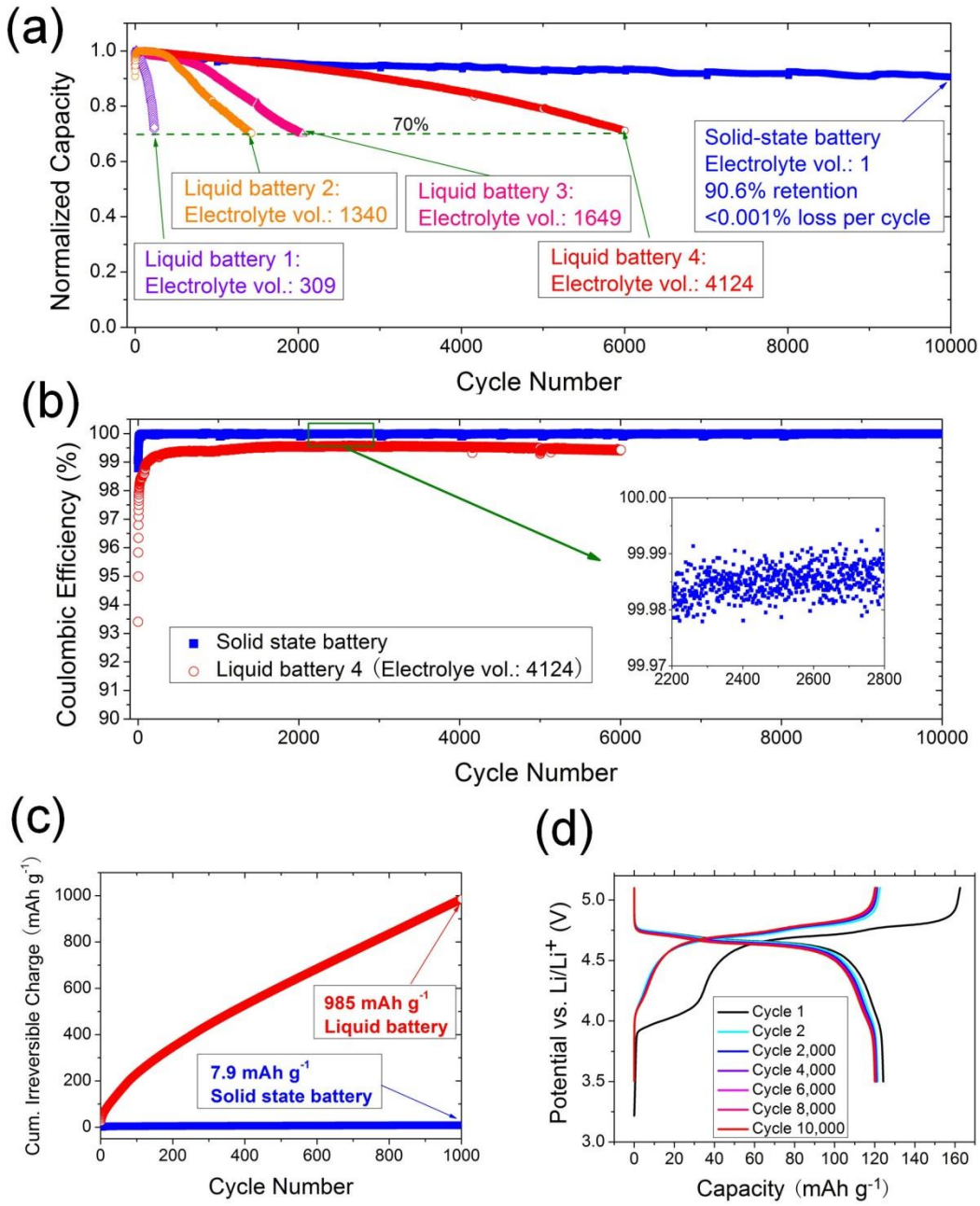

Figure 1. (a) Capacity retention, (b) coulombic efficiency, and (c) cumulative irreversible charge of high-voltage solid-state and liquid-electrolyte lithium batteries. The cathode is $LiNi_{0.5}Mn_{1.5}O_4$ cathode, and the anode is Li metal. Volume of electrolyte is normalized to the volume of the cathode. All cells were cycled under a rate of 5C. (d) Voltage profile of the solid-state battery under C/10.

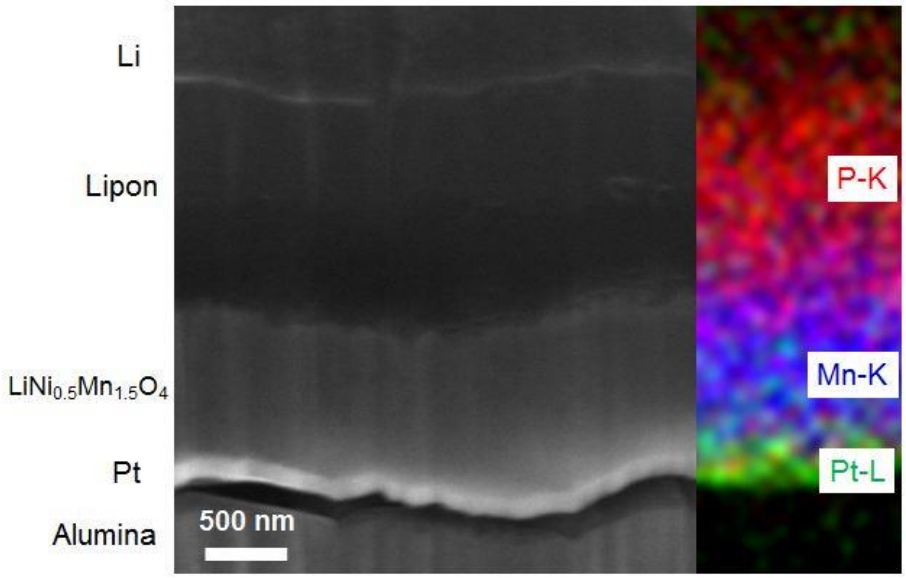

Figure 2. SEM image and EDX elemental mapping of the cross section of the solid-state lithium battery after 1,000 cycles. The de-bonding between the Pt current collector and the alumina substrate is caused by sample preparation using focused ion beam (FIB).

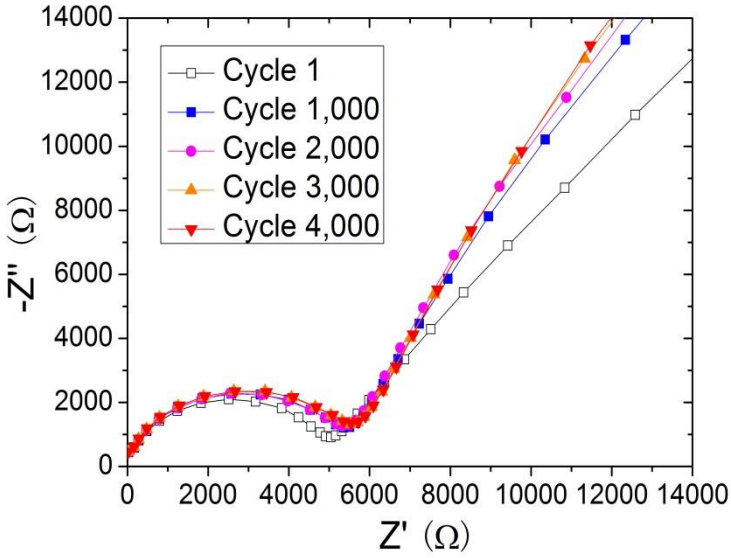

(a)

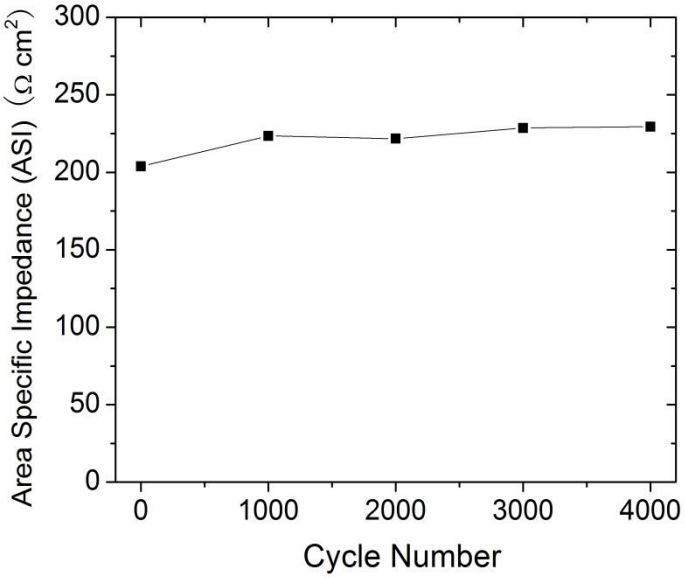

(b)

Figure 3. (a) EIS Nyquist plots of the solid-state battery at 3.5 V at different cycles. (b) Area specific impedance (ASI) at different cycles.

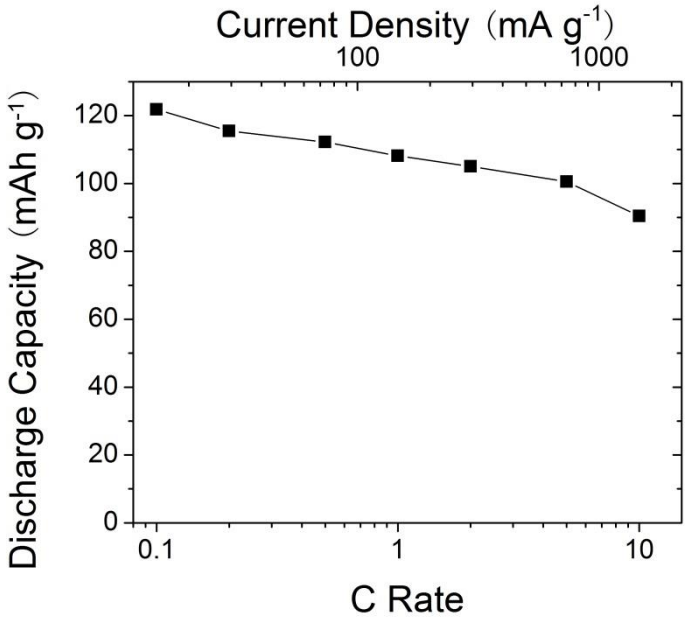

Figure 4. Discharge rate performance of the solid-state battery. Before each measurement, the cell was charged at a slow rate of C/10.

The table of contents entry (50−60 words)

A solid-state high-voltage lithium battery with an operating voltage of ~4.7 V has been demonstrated to deliver a cycle life of 10,000 with 90% capacity retention. The solid electrolyte enables the use of high-voltage cathodes and Li anode with minimum side reaction, leading to a high coulombic efficiency of 99.98%.

Keyword
high-voltage cathode, $LiNi_{0.5}Mn_{1.5}O_4$ spinel, solid electrolyte, lithium-ion battery, solid-state battery

Solid Electrolyte: the Key for High-Voltage Lithium Batteries

Juchuan Li *, Cheng Ma, Miaofang Chi, Chengdu Liang, and Nancy J. Dudney *

ToC figure

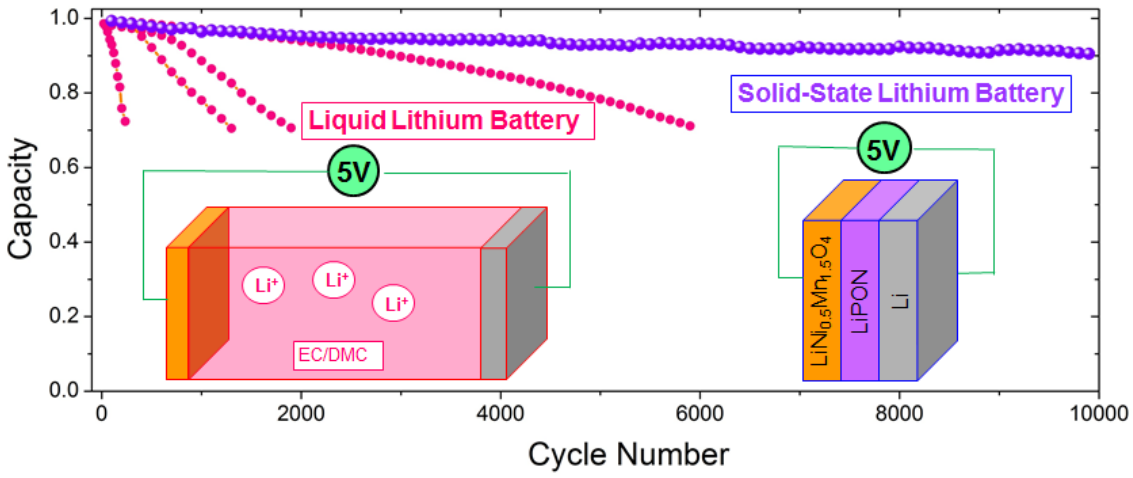

Submitted to ADVANCED ENERGY MATERIALS

Supporting Information

Solid Electrolyte: the Key for High-Voltage Lithium Batteries

*Juchuan Li *, Cheng Ma, Miaofang Chi, Chengdu Liang, and Nancy J. Dudney **

Dr. Juchuan Li, Dr. Nancy J. Dudney
Materials Science & Technology Division, Oak Ridge National Laboratory
Oak Ridge, TN, 37831, USA
Email: lij2@ornl.gov; dudneynj@ornl.gov

Dr. Cheng Ma, Dr. Miaofang Chi, Dr. Chengdu Liang
Center for Nanophase Materials Sciences, Oak Ridge National Laboratory
Oak Ridge, TN, 37831, USA

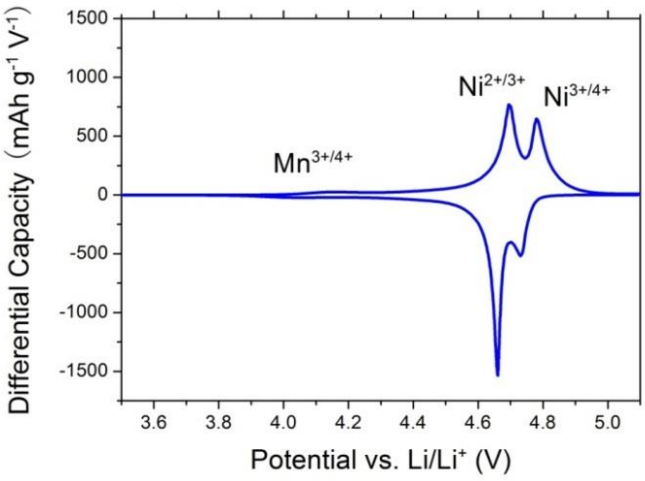

Figure S1. Differential capacity voltage profile of $LiNi_{0.5}Mn_{1.5}O_4$ in solid-state batteries.

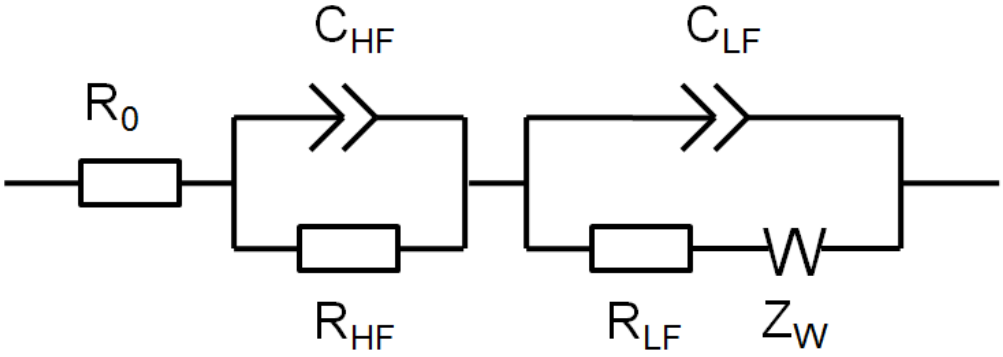

Figure S2. Equivalent circuit for EIS fitting. R_0 represents the resistance of the external circuit and wires. The resistance and capacitance high high frequency (R_{HF} and C_{HF}) is a combined result of interfacial resistance/capacitance and the ionic resistance of Lipon electrolyte and dielectric polarization capacitance. R_{LF} and C_{LF} represents the charge transfer resistance and double layer capacitance, respectively. Z_W is the Warburg elements.

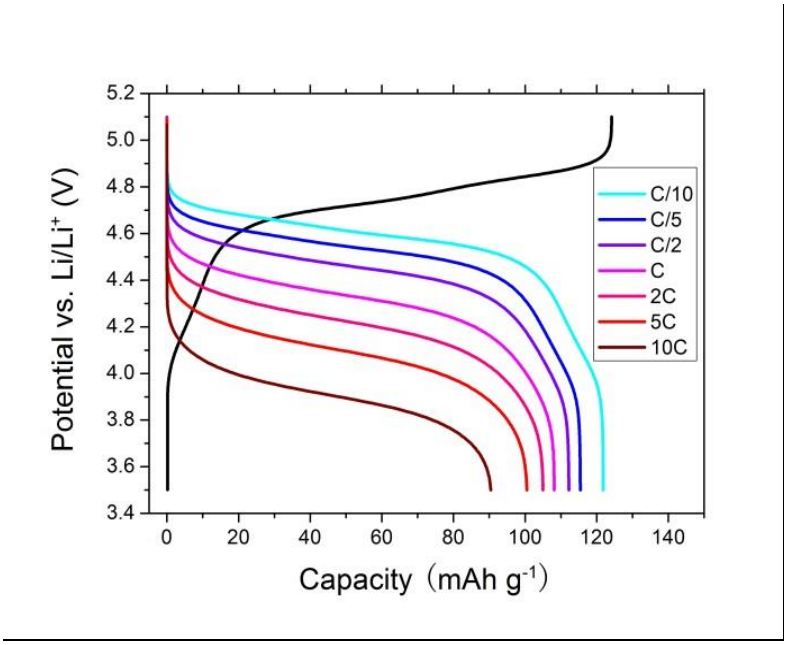

Figure S3. Voltage profiles of the solid-state lithium battery discharged at different rates. The battery was charged at C/10 before each discharge measurement.